Layering of a l iquid metal in contact with a hard wall

Huisman, W.J.; Peters, J.F.; Zwanenburg, M.J.; de Vries, S.A.; Derry, T.E.; Abernathy, D.; van der Veen, J.F.

[Link to publication](#)

3. Partridge, R. B. & Peebles, P. J. E. Are young galaxies visible? *Astrophys. J.* **147**, 868–886 (1967).
4. Toomre, A. in *The Evolution of Galaxies and Stellar Populations* (eds Tinsley, B. M. & Larson, R. B.) 401–416 (Yale Univ. Observatory, New Haven, 1977).
5. Schwezier, F. Colliding and merging galaxies III. The dynamically young merger remnant NGC 3921. *Astron. J.* **111**, 109–129 (1996).
6. Williams, R. E. *et al.* The Hubble Deep Field: observations, data reduction, and galaxy photometry. *Astron. J.* **112**, 1335–1389 (1996).
7. Hogg, D. W., Neugebauer, G., Armus, L., Matthews, K., Pahre, M. A., Soifer, B. T. & Weinberger, A. J. Near infrared imaging of the Hubble Deep Field with the Keck Telescope. *Astron. J.* **113**, 474–482 (1997).
8. Dickinson, M. *et al.* (http://www.stsci.edu/ftp/science/hdf/hdf.html).
9. Moustakas, L. A., Davis, M., Graham, J. R., Silk, J., Peterson, B. & Yoshii, Y. Colors and K-band counts of extremely faint field galaxies. *Astrophys. J.* **475**, 445–456 (1997).
10. Cowie, L. L., Gardner, J. P., Ilu, E. M., Songaila, A., Hodapp, K.-W. & Wainscoat, R. J. The Hawaii K-band galaxy survey. I. Deep K-band imaging. *Astrophys. J.* **434**, 114–127 (1994).
11. Madau, P., Ferguson, H. C., Dickinson, M. E., Giavalisco, M., Steidel, C. C. & Fruchter, A. High-redshift galaxies in the Hubble Deep Field: colour selection and star formation history to z ~ 4. *Mon. Not. R. Astron. Soc.* **283**, 1388–1404 (1996).
12. Steidel, C. C., Giavalisco, M., Dickinson, M. & Adelberger, K. I. Spectroscopy of Lyman break galaxies in the Hubble Deep Field. *Astron. J.* **112**, 352–358 (1996).
13. Cowie, L. L., Songaila, A., Hu, E. M. & Cohen, J. G. New insight on galaxy formation and evolution from Keck spectroscopy of the Hawaii deep fields. *Astron. J.* **112**, 839–864 (1996).
14. Kauffmann, G., Charlot, S. & White, S. D. M. Detection of strong evolution in the poulation of early-type galaxies. *Mon. Not. R. Astron. Soc.* **283**, L117–L122 (1996).
15. Lilly, S. J., Tresse, L., Hammer, F., Crampton, D. & LeFevre, O. The Canada–France Redshift Survey. VI. Evolution of the galaxy luminosity function to z~1. *Astrophys. J.* **455**, 108–124 (1995).
16. Worthey, G., Faber, S. M. & Gonzalez, J. J. *Astrophys. J.* **398**, 69–73 (1992).
17. Ashman, K. M. & Zepf, S. E. *Globular Cluster Systems* (Cambridge University Press, in the press).
18. Gardner, J. P., Sharples, R. M., Frenk, C. S. & Carrasco, B. E. A wide field K-band survey. The luminosity function of galaxies. *Astrophys. J.* **480**, L99–L103 (1997).
19. Ellis, R. S. Faint blue galaxies. *Ann. Rev. Astron. Astrophys.* (in the press).
20. Djorgovski, S. G. in *New Light on Galaxy Evolution* (eds Bender, R. & Davies, R. L.) 277–286 (Kluwer, Dordrecht, 1996).
21. Meurer, G., Heckman, T. M., Lehnert, M. D., Leitherer, C. & Lowenthal, J. The panchromatic starburst intensity limit at low and high redshift. *Astron. J.* **114**, 54–68 (1997).
22. Zepf, S. E. & Silk, J. On the effects of bursts of massive star formation during the evolution of ellipitcal galaxies. *Astrophys. J.* **466**, 114–121 (1996).
23. Baugh, C. M., Cole, S. & Frenk, C. S. Evolution of the Hubble sequence in hierarchical models for galaxy formation. *Mon. Not. R. Astron. Soc.* **283**, 1361–1378 (1996).
24. Cole, S., Aragon-Salamanca, A., Frenk, C. S., Navarro, J. F. & Zepf, S. E. A recipe for galaxy formation. *Mon. Not. R. Astron. Soc.* **271**, 781–806 (1994).
25. Kauffmann, G., Guiderdoni, B. & White, S. D. M. Faint galaxy counts in a hierarchical universe. *Mon. Not. R. Astron. Soc.* **267**, 981–999 (1994).
26. Madau, P. Radiative transfer in a clumpy universe: the colors of high-redshift galaxies. *Astrophys. J.* **441**, 18–27 (1995).
27. Bertin, E. & Arnouts, S. SExtractor: software for source extraction. *Astron. Astrophys. Suppl. Ser.* **117**, 393–404 (1996).

Layering of a liquid metal in contact with a hard wall

**Willem Jan Huisman*, Joost F. Peters§,
Michel J. Zwanenburg§, Steven A. de Vries*,
Trevor E. Derry†, Douglas Abernathy‡
& J. Friso van der Veen§**

* *FOM-Institute for Atomic and Molecular Physics, Kruislaan 407, 1098 SJ Amsterdam, The Netherlands*

† *Schonland Research Centre for Nuclear Sciences, University of Witwatersrand, Private Bag 3, P.O. Wits, 2050 Johannesburg, South Africa*

‡ *European Synchrotron Radiation Facility, BP 220, 38043 Grenoble Cedex, France*

§ *University of Amsterdam, Van der Waals-Zeeman Institute, Valckenierstraat 65, 1018 XE Amsterdam, The Netherlands*

When a liquid makes contact with a solid wall, theoretical studies[1–4] indicate that the atoms or molecules will become layered adjacent to the wall, giving rise to an oscillatory density profile. This expectation has not, however, been directly verified, although an oscillatory force curve is seen for liquids compressed between solid surfaces[5]. Here we present the results of an X-ray scattering study of liquid gallium metal in contact with a (111) diamond surface. We see pronounced layering in the liquid

density profile which decays exponentially with increasing distance from the wall. The layer spacing is about 3.8 Å, which is equal to the repeat distance of (001) planes of upright gallium dimers in solid α-gallium. Thus it appears that the liquid near the wall assumes a solid-like structure similar to the α-phase, which is nucleated on freezing at lower temperatures. This kind of ordering should significantly influence flow, capillary osmosis, lubrication and wetting properties[5,6], and is likely to trigger heterogeneous nucleation of the solid.

Wall-induced oscillations in the atomic density are difficult to detect because they occur at a deeply buried interface over a depth interval of typically less than a nanometre. An earlier study of an electrolyte–silver (111) interface showed layering of the water molecules close to the electrode[7]. This ordering phenomenon, however, relates to the presence of a strong electric field at the interface, causing the dipolar water molecules to be preferentially oriented and attracting them to the silver surface. For the free surfaces of liquid Hg and Ga, the in-plane pair distribution function[8] and the density profile along the surface normal[9,10] have been determined. In the latter case the strong gradient in the density dependent one-body potential across the liquid–vapour interface, which acts as an effective force on the surface ion cores, is responsible for a layering effect[25]. The layering reported here is present in a nonpolar elemental liquid lying against a hard wall, in the absence of an external field. This reflects the commonly occurring situation of having a liquid metal contained in a crucible.

Our choice of materials is convenient for several reasons: Ga is liquid at 300 K (supercooled by 8 K) and diamond is essentially
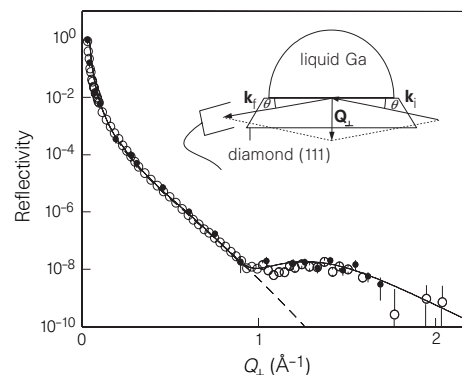

Figure 1 Reflectivity of the Ga/diamond (111) interface as a function of perpendicular momentum transfer $Q_\perp$. Measured reflectivities obtained from transverse momentum scans and θ–2θ scans are represented by filled and open circles, respectively. The solid curve is the best-fit reflectivity curve, obtained by Fourier transform of the electron density profile of Fig. 2; see also equation (1). The dashed curve is a model calculation for a non-oscillatory density profile, see text. The inset shows a schematic of the scattering geometry. The incoming beam is represented by the wavevector $\mathbf{k}_i$, the outgoing beam by $\mathbf{k}_f$. The interface is illuminated from the substrate side with the monochromatic X-ray beam. The top surface of the liquid and the bottom surface of the substrate are shielded from the incoming beam. After scattering, the photons travel through the crystal again on their way to the detector. The momentum transfer $\mathbf{Q}$, the difference between the wavevectors of the incident and scattered photons, is normal to the interface. Note that the index of refraction of Ga is smaller than that of diamond. As the cross section of carbon for Compton scattering is relatively large and a significant volume of bulk liquid is illuminated, there is a high background of diffuse scattering. For the highest momentum transfers, the signal-to-background ratio is a few per cent. At a photon energy of 17 keV, the beam is attenuated by a factor of four along the total pathlength travelled in the diamond. The data were corrected for a 12% variation in the attenuation over the $Q_\perp$ range covered. These experiments have only become feasible because third-generation synchrotron sources deliver such brilliant beams of energetic X-rays that sufficient count-rates can be obtained from the small ordering effects in a few atomic layers.

transparent to X-rays at the photon energy used (17 keV), enabling the incident beam to reach the interface from the diamond side (inset of Fig. 1). The diamond (111) substrate, having a high surface free energy, is a prototypical hard wall, which at 300 K is nonreactive towards Ga and is stable against bond breaking[11]. However, the preparation of an atomically clean interface requires a special procedure involving the controlled deposition, in an ultrahigh vacuum (UHV) environment, of a drop of liquid metal free of surface oxide onto a horizontally positioned clean substrate. The X-ray scattering experiment is to be done *in situ*, so that contaminants from the ambient will not be absorbed by the liquid drop. We have constructed a dedicated UHV set-up which fulfils all of these requirements[26]. The set-up is fitted with a cylindrical Be-window which is transparent to X-rays and provides access to a large portion of reciprocal space.

The C(111) substrate was a synthetic, type-Ib diamond crystal, of which the surface ($\sim 41\,mm^2$) was abrasively and manually polished[12]. The polished surface had a small misorientation with respect to the (111) plane; its normal tilted by 0.3° towards the [100] azimuthal direction. Subsequent flash-heating in the UHV set-up to 1,000 °C resulted in an atomically clean (2×1)-reconstructed surface[12]. A millimetre-sized drop of liquid Ga (99.9999% purity) was deposited onto the diamond surface by gently pushing the plunger of a Ga-filled alumina 'syringe' positioned directly above the surface[13]. The first drops from a fresh load usually have an oxide skin. We therefore deposited them in a tantalum drip tray which can be rotated in front of the surface. After three or four drops, the Ga drops were atomically clean, as was checked earlier by Auger electron spectroscopy in a separate apparatus. We then retracted the tray and deposited a clean drop onto the surface. The wetting angle was found to be 116(6)° and the contact area 9 mm², as measured *in situ* by X-ray transmission and reflection.

The X-ray scattering measurements were made at the undulator beamline ID10 of the European Synchrotron Radiation Facility in Grenoble, France[14]. A wavelength of 0.727 Å (energy 17.058 keV) was selected. The scattered intensities were measured using a NaI scintillation detector behind slits defining the momentum acceptance to be $0.02\,Å^{-1}$ and $0.07\,Å^{-1}$ in the horizontal and vertical directions, respectively. Specular reflectivity measurements were made for perpendicular momentum ($Q_\perp$) transfers in the range $0 < Q_\perp < 2.1\,Å^{-1}$. Different values of $Q_\perp$ within this range were

selected by tilting the chamber through an angle θ with respect to the horizontal plane and setting the detector at an angle 2θ. At each $Q_\perp$ value, the reflectivity was determined by integrating the scattered intensity in a transverse momentum scan either in the plane of specular reflection or perpendicular to this plane. Such scans enable us to subtract from the signal the intrinsic background arising from elastic diffuse scattering from the Ga bulk liquid[9,10]. In addition, symmetric $\theta-2\theta$ scans were made at the specular peak and in the background at either side of the peak. Over the entire $Q_\perp$ range the peaks in the transverse scans were found to have a constant width determined by the instrumental resolution, indicating that we have integrated over the true specular intensity only. It was checked that the three procedures, after usual corrections for illuminated area, Lorentz factor and slit settings[15], yielded the same specular reflectivity values to within 10%.

The measured specular reflectivity, shown in Fig. 1 as a function of $Q_\perp$, shows a broad oscillation with a maximum at $\sim 1.5\,Å^{-1}$. This is a signature of layerwise ordering in the liquid with a period of $2\pi/1.5 = 4\,Å$. In search for the best fit to the data we have considered a variety of density profiles across the interface. For each model, we calculate the specularly reflected fraction $R(Q_\perp)$ of the incoming flux within the Born approximation using the equation

$$R(Q_\perp) = \left(\frac{4\pi r_e}{Q_\perp}\right)^2$$
$$\times \left| \int_{-\infty}^{\infty} \left[f^C(Q_\perp)\rho^C(z) + f^{Ga}(Q_\perp)\rho^{Ga}(z) \right] \exp(iQ_\perp z)dz \right|^2 \quad (1)$$

where $f^C(Q_\perp)$ and $f^{Ga}(Q_\perp)$ are the atomic form factors and $\rho^C(z)$ and $\rho^{Ga}(z)$ the in-plane averaged atomic density distributions for diamond and Ga; r_e is the classical electron radius. In the model, which has in total five adjustable parameters, Ga layers are represented by gaussian functions of increasing width on top of a solid substrate represented by an error function. This yields a damped oscillatory density profile close to the interface and a uniform density far away at either side.

The discrete layer structure of the diamond crystal is not incorporated in the model. Because of the miscut, the normal of the physical interface makes a small angle with the line in reciprocal space that connects the bulk Bragg peaks from the diamond crystal.
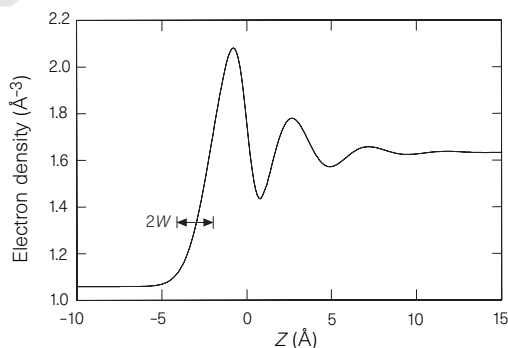

Figure 2 The top panel shows the best-fit model of the oscillatory in-plane averaged electron density profile as a function of the distance z along the interface normal. Far away from the interface, the electron density distributions correspond to the bulk diamond atomic density of 1.77×10^{23} atoms per cm³ and the bulk liquid Ga atomic density of 5.27×10^{22} atoms per cm³. The panel below shows in projection a structural model consistent with the above density profile. Carbon atoms are illustrated by small circles and Ga atoms by larger ones; Ga$_2$ dimers are represented by two atoms connected by a line. Also drawn are the characteristic five- and seven-membered rings of the π-bonded chain reconstruction of the diamond (111) surface. The model features an accumulation of oriented Ga$_2$ dimers in increasingly disordered (001) planes of α-Ga. As indicated by the vertical lines, the planes of oriented dimers correspond to successive regions of high electron density (where the dimer ends meet) and of low electron density (at the centre of each dimer).

Therefore, in our $Q_\perp$ scans we do not encounter the first Bragg peak at $|Q| = 3\,\text{Å}^{-1}$ and its tail at smaller Q values[16].

The best fit for the data is obtained for the decaying oscillatory density profile shown in Fig. 2. The oscillation period in the Ga profile equals 3.83 Å. This distance coincides with the distance between two consecutive (001) planes of almost upright oriented Ga_2 dimers in solid α-Ga, which is the stable solid phase of Ga at low temperature and ambient pressure[17]. The layering extends into the bulk liquid with a $1/e$-decay depth of 4 Å. The areal density of the first layer is larger than that of bulk liquid Ga by 7%. The interface has an overall root mean square (r.m.s.) width W of 1.2 Å (indicated in Fig. 2), which agrees well with the gaussian r.m.s. roughness of 1.4 Å previously measured on the same substrate but without Ga on top[27]. Also the (2×1) reconstruction seems to be preserved underneath the Ga droplet, as is evident from a striking similarity between non-specular reflectivity curves from both surfaces. The Ga liquid seems to replicate the morphology of the diamond surface. A schematic representation of our model for the layered liquid on top of the (2×1) reconstructed diamond (111) surface is given in Fig. 2.

We have considered other possible structural models for the diamond–Ga interface. For example, specific distributions of atomic step disorder at the interface may give rise to oscillations in the reflectivity[16]. However, we measured non-specular reflectivity curves on both Ga-covered and clean surfaces (not shown) but found no such oscillations. Instead, we find for both surfaces identical monotonically decaying Bragg tails for momentum transfers up to $1.5\,\text{Å}^{-1}$ (midway between two bulk Bragg points). Within this range of momentum transfers the step disorder can be accounted for by a Debye–Waller factor which includes a gaussian roughness of 1.1 Å. To show the effect of step disorder we include in Fig. 1 a specular reflectivity curve calculated for an interface with no density oscillations at the liquid side. Such curves do not describe the measurements. Another model featuring a uniform liquid boundary layer of a different density only gives a reasonable fit to the data if a 7 Å thick layer of at least 20% higher atomic density is assumed, which is clearly unphysical. Density profiles with layer spacings from solid phases of Ga other than α-Ga do not describe the data either. The predominant nearest-neighbour distance of 2.56 Å present in liquid Ga (ref. 18) yields a reflectivity maximum at $Q_\perp = 2.5\,\text{Å}^{-1}$, which is outside the range of measurement. At these high $Q_\perp$ values the intrinsic background from the bulk liquid and the crystal becomes too large.

The decay length of the layering amplitude is roughly equal to that of the pair correlation function for bulk Ga (ref. 18). This indicates that short-range order in bulk liquid Ga and layering at the interface are closely related, even though the layering period is different. It supports the notion that the formation of layers is a geometrical consequence of the requirement to form a sharp interface imposed by the diamond wall. The value of 4 Å found by us is smaller than the large value of 5.8 Å found for the decay depth of surface-induced monoatomic layers at the free Ga surface[10].

We believe that layering of the Ga liquid into a structure similar to that in (001) planes of α-Ga is sterically favoured. Liquid Ga is known to contain a non-negligible concentration of Ga_2 dimers in the bulk, which is a manifestation of a certain degree of covalency in the bonding (interatomic distance of 2.44 Å)[17,19]. The dimers accumulate at the diamond $(111)-2 \times 1$ substrate in nearly upright position, thus forming a few solid-like (001) planes of α-Ga. A possible driving mechanism for this type of interfacial segregation and orientational ordering of dimers is an energy gain in the interfacial bonding resulting from the nearly perfect match (<3%) in distance between adjacent π-bonded chains of atoms in the (2×1) reconstructed diamond (111) substrate and the zigzag arrangement of dimers in α-Ga(001) planes. We note, however, that the energy gain is probably small, because the bonding between Ga and diamond is relatively weak, as judged from the large wetting angle of 116°. Also favourable for the accumulation of dimers may

be the fact that this makes the transition across the interface from metallic to covalent bonding less abrupt.

The observed layering of liquid Ga against diamond (111) may have implications for our general understanding of freezing transitions in atomic metals and highlights the possible role of the container wall in triggering the crystallization. Of all crystal faces on α-Ga, the (001) face has the highest atomic density and is the one most stable against surface melting[20,21]. It is also known that in a supercooled liquid, the barrier for freezing is smallest against the most dense crystal face[22]. It is therefore tempting to interpret the observed layering as an atomic-scale manifestation of interfacial freezing. However, contrary to the case of surface melting[23], which pre-empts superheating of the crystal, the interfacial freezing observed is not effective in pre-empting supercooling of the liquid. Apparently, an energetic barrier for bulk freezing remains present, making the interfacial freezing a case of incomplete 'wetting' of the melt by the crystal. An energetic barrier has been attributed earlier to an entropy loss associated with the layering[24]. The possible effects of the enhanced ordering at the interface on the barrier to heterogeneous freezing and on the maximum supercooling interval warrant further investigation. Measurements of the temperature dependence of the layering effect may help us to resolve this issue. □

1. McMullen, W. E. & Oxtoby, D. W. A density functional approach to freezing transitions in molecular fluids: dipolar hard spheres. *J. Chem. Phys.* **88,** 4146–4156 (1987).
2. Curtin, W. A. Density-functional theory of the solid–liquid interface. *Phys. Rev. Lett.* **59,** 1228–1231 (1987).
3. Sikkenk, J. H., Indekeu, J. O., van Leeuwen, J. M. J. & Vossnack, E. O. Molecular-dynamics simulation of wetting and drying at solid–fluid interfaces. *Phys. Rev. Lett.* **59,** 98–101 (1987).
4. Ma, W.-J., Banavar, J. R. & Koplik, J. A molecular dynamics study of freezing in a confined liquid. *J. Chem. Phys.* **97,** 485–493 (1992).
5. Bhushan, B., Israelachvili, J. N. & Landman, U. Nanotribology: friction, wear and lubrication at the atomic scale. *Nature* **374,** 607–609 (1995).
6. Derjaguin, B. V. & Churaev, N. V. Structure of the boundary layers of liquids and its influence on the mass transfer in fine pores. *Progr. Surf. Mem. Sci.* **14,** 69–130 (1981).
7. Toney, M. F. *et al.* Voltage-dependent ordering of water molecules at an electrode–electrolyte interface. *Nature* **368,** 444–446 (1994).
8. Barton, S. W. *et al.* Distribution of atoms at the surface of liquid mercury. *Nature* **321,** 685–687 (1986).
9. Magnussen, O. M. *et al.* X-ray reflectivity measurements of surface layering in liquid mercury. *Phys. Rev. Lett.* **74,** 4444–4447 (1995).
10. Regan, M. J. *et al.* Surface layering in liquid gallium: an X-ray reflectivity study. *Phys. Rev. Lett.* **75,** 2498–2502 (1995).
11. Pate, B. B. The diamond surface: atomic and electronic structure. *Surf. Sci.* **165,** 83–142 (1986).
12. Derry, T. E., Smit, L. & van der Veen, J. F. Ion-scattering determination of the atomic arrangement at polished diamond(111) surfaces before and after reconstruction. *Surf. Sci.* **167,** 502–518 (1986).
13. Norris, C. & Wotherspoon, J. T. M. The optical density of states of liquid gallium. *J. Phys.* F**7,** 1599–1606 (1977).
14. Grübel, G., Als-Nielsen, J. & Freund, A. K. The Troika beamline at ESRF. *J. Physique IV* **4,** C9, 27–34 (1994).
15. Vlieg, E. Integrated intensities using a six-circle X-ray diffractometer. *J. Appl. Crystallogr.* **30,** 532–543 (1997).
16. Lagally, M. G., Savage, D. E. & Tringides, M. C. in *Reflection high-energy electron diffraction and reflection imaging of surfaces* 139–174 (Plenum, New York, 1988).
17. Defrain, A. États métastables du gallium. Surfusion et polymorphisme. *J. Chim. Phys.* **74,** 851–862 (1977).
18. Narten, A. H. Liquid gallium: comparison of X-ray data and neutron-diffraction data. *J. Chim. Phys.* **56,** 1185–1189 (1972).
19. Gong, X. G., Chiarlotti, G. L, Parrinello, M. & Tosatti, E. Coexistence of monoatomic and diatomic molecular fluid character in liquid gallium. *Europhys. Lett.* **21,** 469–475 (1993).
20. Trittibach, R., Grütter, Ch. & Bilgram, J. H. Surface melting of gallium single crystals. *Phys. Rev.* B**50,** 2529–2536 (1994).
21. Züger, O. & Dürig, U. Atomic structure of the α-Ga(001) surface investigated by STM: direct evidence for the existence of Ga_2 molecules in solid gallium. *Ultramicroscopy* **42–44,** 520–527 (1992).
22. Turnbull, D. Formation of crystal nuclei in liquid metals. *J. Appl. Phys.* **21,** 1022–1028 (1950).
23. Van der Veen, J. F., Pluis, B. & Denier van der Gon, A. W. in *Chemistry and Physics of Solid Surfaces VII* 455–490 (Springer, Berlin, 1988).
24. Turnbull, D. in *Physics of Non-crystalline Solids* 41–56 (North-Holland, Amsterdam, 1964).
25. Rice, S. A., Gryko, J. & Mohanty, U. in *Fluid Interfacial Phenomena* 255–342 (Wiley, Chichester, 1986).
26. Huisman, W. J. *et al.* A new X-ray diffraction method for structural investigations of solid-liquid interfaces. *Rev. Sci. Instrum.* **68,** 4169–4176 (1997).
27. Huisman, W. J. *et al.* Evidence for tilted chains on the diamond(111)-2 × 1 surface. *Surf. Sci.* (in the press).

Correspondence should be addressed to J.F.v.d.V. (e-mail: vdveen@phys.uva.nl).